haematologica
Journal of the Ferrata Storti Foundation

Factor X colocalizes with amyloid light chain deposits in AL amyloidosis: evidence from three patients

by Sénadé Atsou, Alexia Rinsant, Caterina Casari, Peter J Lenting, Vincent Javaugue, Estelle Desport, Laurent Macchi, Cécile V. Denis, Frank Bridoux and Olivier D. Christophe

Received: January 27, 2026.
Accepted: May 7, 2026.

Citation: Sénadé Atsou, Alexia Rinsant, Caterina Casari, Peter J Lenting, Vincent Javaugue, Estelle Desport, Laurent Macchi, Cécile V. Denis, Frank Bridoux and Olivier D. Christophe. Factor X colocalizes with amyloid light chain deposits in AL amyloidosis: evidence from three patients.
Haematologica. 2026 May 14. doi: 10.3324/haematol.2026.300598 [Epub ahead of print]

Factor X colocalizes with amyloid light chain deposits in AL amyloidosis: evidence from three patients

Sénadé Atsou[1], Alexia Rinsant[2], Caterina Casari[1], Peter J Lenting[1], Vincent Javaugue[2], Estelle Desport[2], Laurent Macchi[3], Cécile V Denis[1,4], Frank Bridoux[2†], Olivier D Christophe[1]

[1]Université Paris-Saclay, INSERM, Hémostase Inflammation Thrombose HITh U1176, 94276, Le Kremlin-Bicêtre, France
[2]Service Néphrologie-Hémodialyse-Transplantation Rénale, Centre National de Référence Amylose AL, CHU et Université de Poitiers, 86000, Poitiers, France
[3]Service d'Hématologie Biologique, CRC Maladies hémorragiques constitutionnelles, IRMETIST INSERM 1313, CHU et Université de Poitiers, 86000, Poitiers, France
[4]CHRU de Nancy – 54000 Nancy France
[†]Deceased on August 14, 2025

Running heads: FX Colocalizes with Amyloid Light Chain Deposits

Corresponding author: Olivier D Christophe, PhD; E-mail: olivier.christophe@inserm.fr

Data sharing: Data are available upon reasonable request to the corresponding author

Acknowledgments: We dedicate this manuscript to the memory of Frank Bridoux, whose leadership, insight, and contributions were essential to the conception and execution of this work. We are grateful to Jean-Yves Tinevez from Institut Pasteur, Université Paris Cité, Image Analysis Hub, Paris, France Julien Fernandes from Institut Pasteur, UTechS PBI, C2RT, Paris, France for providing unrestricted access to their facilities, equipment and expertise in microscopic analysis. We also would like to thank the Institut Biomédical du Val-de-Bièvre (IBVB-UMS44), for technically and facility supports.

Funding: This work was supported by the French National Research Agency (Agence Nationale de la Recherche) (grant #ANR-21-CE17-0040-01 to O.D.C.). S.A. was supported by a grant from the French Ministry of Research.

Authors' disclosure: The authors declare no competing financial interests.

Authors' contributions: S.A., A.R., L.M., and O.D.C. performed experiments. S.A., L.M., C.C., C.V.D., P.J.L., F.B., and O.D.C. analyzed data. C.V.D., F.B., and O.D.C. designed and supervised the study. S.A. and O.D.C. wrote the initial version of the manuscript, and all authors contributed to its final editing.

AL amyloidosis (AL) is a rare plasma cell disorder caused by misfolded monoclonal immunoglobulin light chains (LC) that deposit as amyloid fibrils in extracellular matrices.[1] The heart and kidneys are most commonly affected, although hepatic, gastrointestinal, and peripheral nervous system involvement may also occur.[2]

Acquired factor X (FX) deficiency is observed in 8–14% of AL patients[3] and is primarily attributed to FX adsorption onto amyloid fibrils, leading to accelerated clearance. This mechanism is supported by normalization of FX levels following splenectomy, chemotherapy, or autologous stem cell transplantation,[1,2] and by early studies demonstrating rapid clearance of radiolabeled FX and binding to extracted fibrils.[4]

Although fibrils from patients without FX deficiency can bind FX,[5] only one case has reported histological evidence of FX within amyloid deposits.[6]

Thus, despite strong indirect evidence supporting FX adsorption as the principal mechanism of acquired deficiency in AL amyloidosis, direct demonstration of tissue FX sequestration and its relationship to circulating FX activity remains limited and the role of amyloid burden and organ distribution is unclear.

We analyzed tissue biopsies from three AL patients using quantitative immunofluorescence and longitudinally monitoring of FX activity and free LC levels to determine whether tissue-specific FX accumulation correlates with circulating FX activity. Our findings provide new insights into tissue-specific FX accumulation and its relationship with amyloid deposits.

Three patients diagnosed between 2017 and 2020 at the University Hospital of Poitiers were retrospectively included (Supplementary Table S1). The study was approved by the local ethics committee (DR-2011-392) and the Comité de Protection des Personnes (CPP 19.06.06.57922). Hematologic evaluation followed validated criteria[7] and included bone marrow aspiration and serum free light chains (sFLCs) measurement (FreeLite assay). FX, Factor II, and Factor V activities were assessed using standard clotting assays.

Biopsies from minimally invasive sites or affected organs were stained with Congo red and analyzed by immunofluorescence. Analyses were performed on one or multiple biopsy sections per patient, depending on available sites.

Frozen biopsies were sectioned (3 µm), acetone-fixed, blocked, and incubated with primary antibodies against FX, κ, or λ LCs, followed by fluorophore-conjugated secondary antibodies and DAPI. Images were acquired using a Cell Discoverer 7 microscope. Z-stack projections were analyzed with QuPath 0.2.8,[8] with manual autofluorescence correction.

Regions of interest were classified as positive or negative, Colocalization was quantified using a Groovy-scripted adapted from Fiji JACoP[9], to calculate Pearson and Manders coefficients.

Patient IgGs were purified using Protein G columns and tested by ELISA on FX-coated plates.

All experiments were performed in triplicate with appropriate controls. All procedures complied with institutional ethical standards; written informed consent was obtained from all patients.

Patients 1 and 2 had acquired factor X deficiency, defined by decreased factor X coagulant activity (FX:C below the normal range), at diagnosis, whereas Patient 3 had normal FX:C levels (Table S1). All

exhibited typical AL organ involvement. Clonal plasma cells and circulating sFLCs were assessed in bone marrow aspirates and peripheral blood with kappa (κ) chains in Patient and lambda (λ) chains in Patients 2–3.

All patients initially received CyBorD therapy (Table S2). Hematologic responses, assessed by reduction in involved minus uninvolved FLC (dFLC; Figures 1A, 2A, 3A, blue lines), preceded changes in FX activity (red lines). In Patient 1, a very good partial response (VGPR) was followed by delayed FX normalization; a similar pattern occurred after relapse and Dara/Len/Dex therapy. Patient 2 showed delayed hematologic response with incomplete FX recovery. Patient 3 exhibited minimal FX changes despite sequential partial response, VGPR, and complete remission. Overall, FX recovery lagged behind hematologic improvement and depended on baseline FX deficiency.

Congo red-staining confirmed amyloid deposition in all patients (Figures 1B-C, 2B and 3B, E). Distribution included digestive mucosa (Patient 1), salivary glands (Patients 2 and 3), and abdominal fat (Patients 2 and 3). Serial sections were analyzed for LCs and FX, and colocalization was quantified using Manders' coefficients (M1, M2). Fluorescence intensities and coefficients were compared between amyloid-positive and -negative regions.

In Patient 1, κ LC fluorescence intensity was higher in amyloid-positive intestinal regions compared with negative regions (918 ± 612 arbitrary units or a.u. vs 334 ± 204 a.u.; $P < 0.0001$; $n = 37$), as was FX fluorescence (2153 ± 2110 vs. 543 ± 361 a.u.; $P < 0.0001$; Figures 1B-E). Manders' analysis demonstrated strong colocalization of FX with κ LCs and vice-versa (M1: 0.59 ± 0.28 vs. 0.12 ± 0.13; $P < 0.0001$; M2: 0.81 ± 0.19 vs. 0.28 ± 0.14; $P < 0.0001$; Figures 1F). In Patient 2, similar results were observed in salivary gland and abdominal fat, with increased fluorescence for λ LCs (1639 ± 302 vs. 472 ± 51 a.u.; $P < 0.0001$; $n = 15$) and FX (643 ± 136 vs. 434 ± 117 a.u.; $P = 0.0002$) and colocalization coefficients (M1: 0.661 ± 0.099 vs. 0.539 ± 0.106; $P = 0.0068$; M2: 0.467 ± 0.133 vs. 0.159 ± 0.092; $P < 0.0001$), confirming robust FX–LC association (Figures 2B-H). In Patient 3, λ LCs accumulated in amyloid-positive versus negative salivary glands (1373 ± 198 vs. 791 ± 44 a.u.; $P < 0.0001$; $n = 6$), whereas FX did not (583 ± 79 vs. 579 ± 81 a.u.; $P = 0.93$), resulting in absent colocalization (Figure 3B-D). In contrast, abdominal fat showed higher LC and FX fluorescence intensities in amyloid-positive regions (Figures 3E-H), with significantly increased Manders' coefficients ($P < 0.0001$; Figure 3I), indicating partial colocalization.

Overall, FX–LC colocalization was consistent in patients with FX deficiency and variable in the patient without deficiency.

Our study provides direct evidence that acquired FX deficiency in AL amyloidosis is linked to tissue-specific FX sequestration within amyloid deposits correlating with tissue amyloid load rather than circulating FX levels, suggesting that amyloid burden may predict coagulation deficits. Hematologic remission precedes FX normalization, highlighting delayed coagulation factor recovery.

Unlike multiple myeloma, where organ damage is driven by tumor mass or cytokines, AL amyloidosis is directly caused by circulating monoclonal LCs. Treatment aims to suppress their production to limit fibrillogenesis. FX deficiency is classically attributed to adsorption onto amyloid fibrils, leading to accelerated clearance. Early studies demonstrated rapid disappearance of radiolabeled FX and in vitro

binding to extracted fibrils. Our immunofluorescence data extend these observations by demonstrating FX accumulation in amyloid-rich areas (Patients 1 and 2) and tissue-specific colocalization (Patient 3), supporting a central role for amyloid burden and distribution.

The FX depletion selectivity remains incompletely understood. Although other vitamin K–dependent factors share similar properties, they are less frequently reduced,[3] suggesting amyloid–FX interactions. Tissues with high vascular exposure and substantial amyloid burden showed the strongest FX deposition. Patient 3 exhibited partial colocalization despite normal FX activity, suggesting based on a single case that adsorption may occur without overt coagulopathy, with uncertain determinants possibly involving fibril structure, light chain characteristics, and organ-specific factors.

All patients received CyBorD, followed by individualized therapies, achieving variable hematologic responses. FX normalization lagged behind LC reduction by ~12–18 months in FX-deficient patients. This temporal dissociation suggests circulating FX activity reflects not only LC suppression but also persistence of amyloid deposits acting as a "sink." These observations align with reports of delayed FX recovery after therapy[1,2] and with data showing greater FX improvement in patients achieving complete hematologic response.[12]

Immunofluorescence confirmed that Congo red–positive areas were enriched in FX signal, colocalizing with LCs in FX-deficient patients, while alternative deficiency causes were excluded. In Patient 3, partial colocalization in abdominal fat but not salivary glands support the influence of tissue microenvironment and fibril organization on FX binding.

Clinically, FX deficiency may represent a marker of advanced AL, as prior studies linked FX <50% to increased bleeding risk, more severe cardiac involvement, and reduced survival.[13,14] Monitoring FX during treatment may provide complementary prognostic information, reflecting organ recovery and residual amyloid, and assist in bleeding-risk assessment, particularly for invasive procedures.

The delay between hematologic response and FX normalization indicates coagulopathy management should extend beyond hematologic remission, as residual amyloid deposits may continue to sequester FX. The tissue-specific pattern of FX deposition suggests that organ-targeted reduction of amyloid burden could influence FX recovery. The possible interaction between FX and serum amyloid P component[15] warrants further functional investigation of FX–fibril interactions, including evaluation in other amyloidosis subtypes.

This study is limited by small sample size, restricted biopsy material, and lack of quantitative amyloid burden assessment. Future research should assess FX kinetics in larger cohorts, integrate imaging-based amyloid quantification, and explore individualized FX replacement strategies.

In summary, FX deficiency in AL amyloidosis appears mechanistically linked to tissue-specific sequestration within amyloid deposits. Delayed FX recovery underscores the importance of continued coagulation monitoring and individualized management. FX deposition may occur even in patients with normal activity, raising important questions about its potential role as an amyloid burden biomarker.

References

1. Sanchorawala V. Systemic light chain amyloidosis. N Engl J Med. 2024;390(24):2295-2307.
2. Wechalekar AD, Gillmore JD, Hawkins PN. Systemic amyloidosis. Lancet. 2016;387(10038):2641-2654.
3. Abdallah N, Muchtar E, Dispenzieri A, et al. Coagulation Abnormalities in Light Chain Amyloidosis. Mayo Clin Proc. 2021;96(2):377-387.
4. Furie B, Greene E, Furie BC. Syndrome of acquired factor x deficiency and systemic amyloidosis. N Engl J Med. 1977;297(2):81-85.
5. Furie B, Voo L, McAdam KPWJ, Furie BC. Mechanism of factor x deficiency in systemic amyloidosis. N Engl J Med. 1981;304(14):827-830.
6. Tashiro H, Shirasaki R, Watanabe M, et al. Direct Factor X sequestration by systemic amyloid light-chain amyloidosis. Clin Case Rep. 2018;6(3):513-515.
7. Palladini G, Dispenzieri A, Gertz MA, et al. New criteria for response to treatment in immunoglobulin light chain amyloidosis based on free light chain measurement and cardiac biomarkers: impact on survival outcomes. J Clin Oncol. 2012;30(36):4541-4549
8. Bankhead P, Loughrey MB, Fernández JA, et al. QuPath: Open source software for digital pathology image analysis. Sci Rep. 2017;7(1):16878.
9. Bolte S, Cordelières FP. A guided tour into subcellular colocalization analysis in light microscopy. J Microsc. 2006;224(Pt 3):213-232.
10. Diaz-Pallares C, Lee H, Luider J, et al. Cyclophosphamide, Bortezomib and Dexamethasone (CyBorD) for the treatment of newly diagnosed AL amyloidosis: impact of response on survival outcomes. Clin Lymphoma Myeloma Leuk. 2020;20(6):394-399.
11. Toenges R, Steinmann J, Siegemund A, et al. Acquired Factor X deficiency in systemic light chain amyloidosis: Factor X recovery after bleeding complications, splenectomy, chemotherapy and remission. Blood. 2017;130(Supplement 1):4892.
12. Gao Y, Shen K, Chang L, et al. Prevalence, clinical characteristics and treatment outcome of factor X deficiency in a consecutive cohort of primary light-chain amyloidosis. Leuk Res. 2022;120:106917.
13. Iglay K, Aldridge ML, Calcinai M, Wolford E, Ashrani AA. The global epidemiology of acquired factor X deficiency. Hematology. 2025;30(1):2476254.
14. Patel G, Hari P, Szabo A, et al. Acquired factor X deficiency in light-chain (AL) amyloidosis is rare and associated with advanced disease. Hematol Oncol Stem Cell Ther. 2019;12(1):10-14.
15. Muczynski V, Aymé G, Regnault V, et al. Complex formation with pentraxin-2 regulates factor X plasma levels and macrophage interactions. Blood. 2017;129(17):2443-2454.

Figure Legends

Figure 1

Longitudinal dynamics of factor X activity and colocalization with amyloid deposits in Patient 1.

(A) Longitudinal monitoring of factor X (FX) activity (%) and the difference between involved and uninvolved serum free light chains (dFLC, mg/L) during treatment. Left axis: FX (%); right axis: dFLC (mg/L). Blue line: dFLC concentration; red line: FX activity. Numbers indicate successive therapies: 1 = CyBorD (9 cycles, 8 months), 2 = daratumumab/lenalidomide/dexamethasone (6 months), 3 = daratumumab/dexamethasone (6 months). dFLC levels decreased rapidly following treatment initiation, whereas FX activity increased only after a lag period (~12–18 months).

(B, C) 63× photomicrographs of Congo red-stained sections under polarized light showing amyloid-positive regions (apple-green birefringence) in the antre (B) and colon (C). Lower white boxes indicate areas rich in amyloid deposits (white arrows), whereas upper boxes indicate amyloid-negative areas.

(D) Wide-field immunofluorescence in the antre showing kappa FLC (green) and FX (red); co-localization appears yellow (63× objective; scale bars, 500 µm).

(E) Comparison of mean fluorescence intensity (mean gray value) for each channel, with green representing kappa FLC and red representing FX, between Congo red (CR)–positive (+) and CR–negative (–) fields (n = 37; data shown as individual fields with mean ± SD; unpaired t-test).

(F) Manders coefficients (M1, M2) indicating significantly higher co-localization of FX with kappa FLC (M1) and vice versa (M2) in amyloid-rich versus negative areas ($P < 0.0001$).

Figure 2

Longitudinal dynamics of factor X activity and colocalization with amyloid deposits in Patient 2.

(A) Longitudinal monitoring of FX activity (%) and dFLC concentrations (mg/L). Left axis: FX (%); right axis: dFLC (mg/L). Blue line: dFLC concentration; red line: FX activity. Numbers indicate therapies: 1 = CyBorD (6 cycles, 6 months), 2 = BorD + lenalidomide (6 months), 3 = not used. The initial dFLC response was delayed, and FX activity increased slowly, remaining below normal despite hematologic remission.

(B) Congo red staining of salivary gland tissue showing amyloid-positive (upper right box, with amyloid structures indicated by white arrows) and amyloid-negative (lower right box) areas.

(C, F) Immunofluorescence of FX (red) and lambda FLC (green) in salivary gland (C) and abdominal fat (F) (63× objective; scale bars, 500 µm). Positive regions show strong co-localization, whereas negative regions show minimal signal.

(D, G) Quantification of fluorescence intensities showing mean gray values of lambda FLC (green) and

FX (red) in positive versus negative fields (n = 15; data shown as individual fields with mean ± SD; unpaired t-test).
(E, H) Manders coefficients (M1, M2) demonstrating significantly higher co-localization of FX with lambda FLC and vice versa in CR-positive versus negative areas (P = 0.0068 and P < 0.0001, respectively).

Figure 3

Longitudinal dynamics of factor X activity and colocalization with amyloid deposits in Patient 3.

(A) Longitudinal monitoring of FX activity (%) and dFLC (mg/L) during successive therapies. Left axis: FX (%); right axis: dFLC (mg/L). Blue line: dFLC concentration; red line: FX activity. Numbers indicate therapies: 1 = CyBorD (6 cycles, 6 months), 2 = BorD + lenalidomide, 3 = BorD + venetoclax. dFLC levels progressively decreased to complete remission, while FX activity remained within the normal range.
(B, E left) Congo red staining of salivary gland (B) and abdominal fat (E, left) biopsies under polarized light, showing apple-green birefringence indicative of amyloid deposits.
(C, E right, F, G) Wide-field fluorescence microscopy of FX (red) and lambda FLC (green) in salivary gland (C) and abdominal fat (E right, F, G) sections (63× objective; scale bars, 500 µm). White (C) and red (E) boxes indicate Congo red–positive areas corresponding to panels (C) and (F), respectively, whereas blue boxes (E) indicate Congo red–negative regions corresponding to panel (G).
(D) Quantification of fluorescence intensity (mean gray value) of lambda FLC (green) and FX (red) in Congo red–positive (+) and negative (–) areas (n = 6 fields), showing no FX accumulation in salivary gland amyloid deposits.
(H) Quantification of fluorescence intensity in abdominal fat (n = 11 fields): green channel (lambda FLC), 1029 ± 190 a.u. vs. 679 ± 88 a.u., P < 0.0001; red channel (FX), 887 ± 385 a.u. vs. 646 ± 177 a.u., P = 0.0520.
(I) Co-localization analysis of FX and lambda FLC using Manders coefficients (M1, M2), showing higher co-localization in Congo red–positive (+) versus negative (–) areas (M1 = 0.45 ± 0.19 vs. 0.12 ± 0.14, P = 0.0004; M2 = 0.85 ± 0.14 vs. 0.17 ± 0.16, P < 0.0001; n = 11). Data are shown as individual fields with mean ± SD (unpaired t-test).

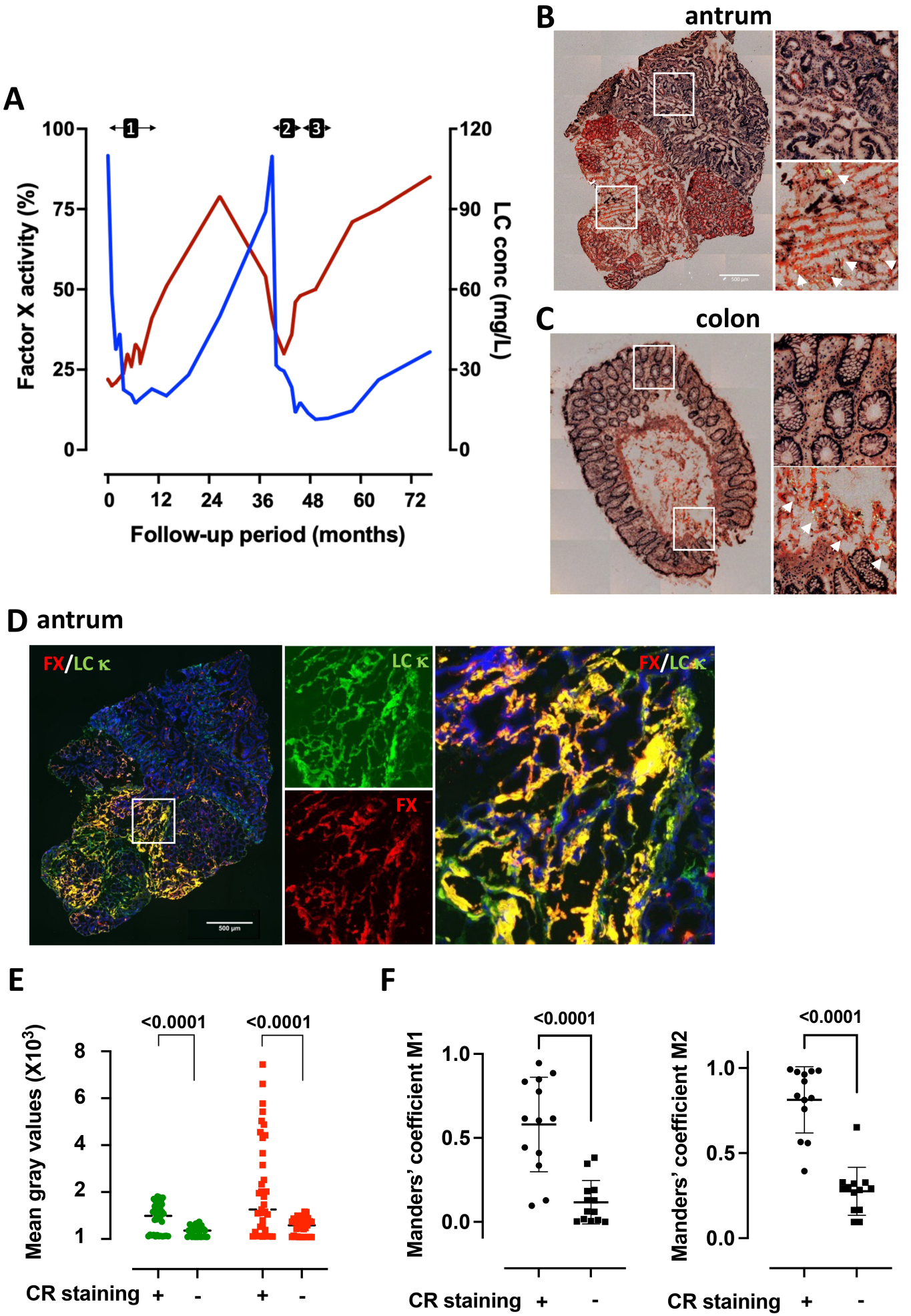
A
100
75
50
25
0
120
90
60
30
0
1
2
3
Factor X activity (%)
LC conc (mg/L)
0
12
24
36
48
60
72
Follow-up period (months)
B
antrum
C
colon
D antrum
FX/LC κ
LC κ
FX
FX/LC κ
500 µm
E
<0.0001
<0.0001
Mean gray values (X10³)
8
6
4
2
1
CR staining + - + -
F
<0.0001
Manders' coefficient M1
1.0
0.5
0.0
CR staining + -
<0.0001
Manders' coefficient M2
1.0
0.5
0.0
CR staining + -

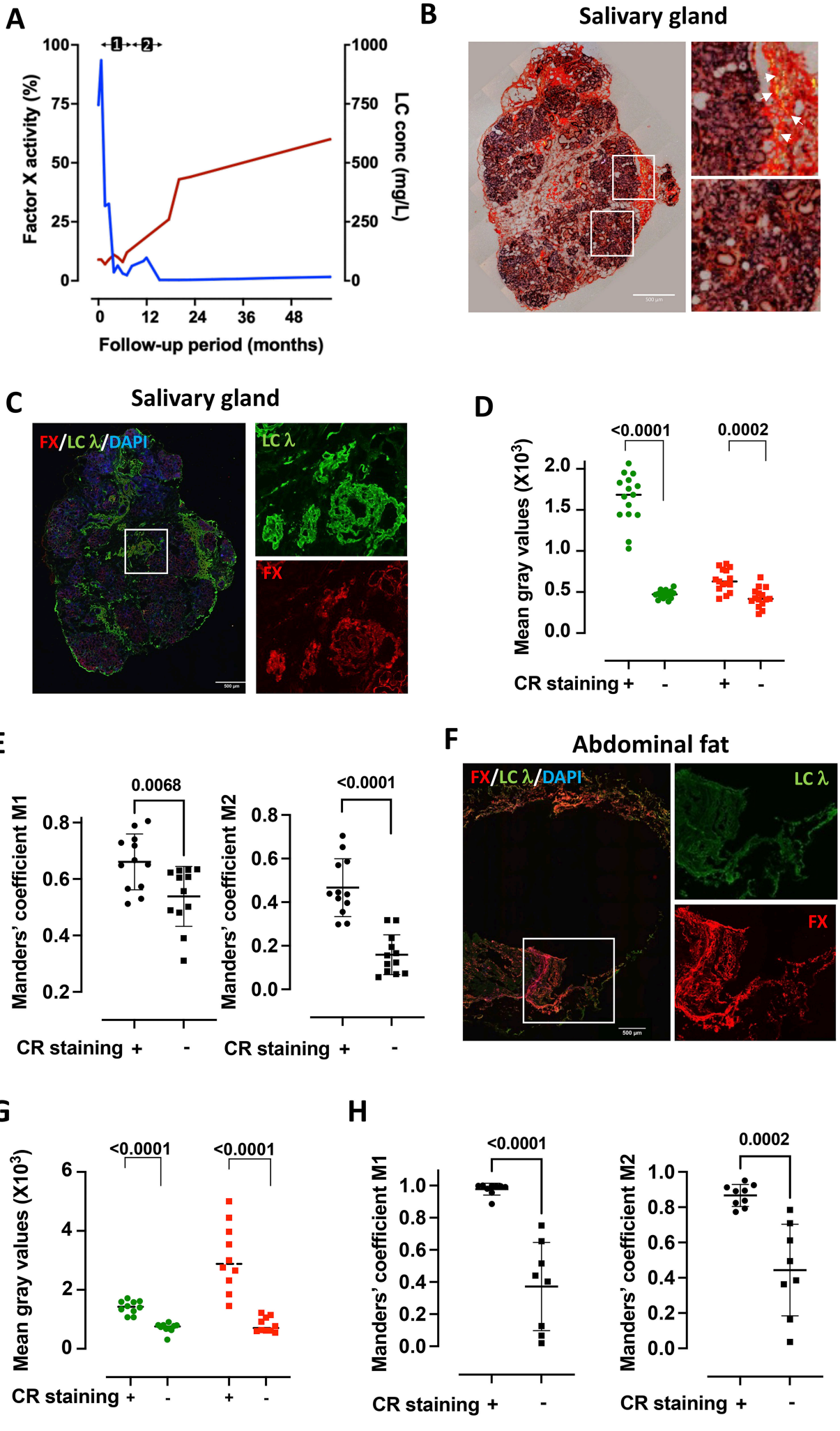
A
Factor X activity (%)
LC conc (mg/L)
Follow-up period (months)
B
Salivary gland
C
Salivary gland
FX/LC λ/DAPI
LC λ
FX
D
Mean gray values (X10³)
<0.0001
0.0002
CR staining + - + -
E
Manders' coefficient M1
Manders' coefficient M2
0.0068
<0.0001
CR staining + -
F
Abdominal fat
FX/LC λ/DAPI
LC λ
FX
G
Mean gray values (X10³)
<0.0001
<0.0001
CR staining + - + -
H
Manders' coefficient M1
Manders' coefficient M2
<0.0001
0.0002
CR staining + -

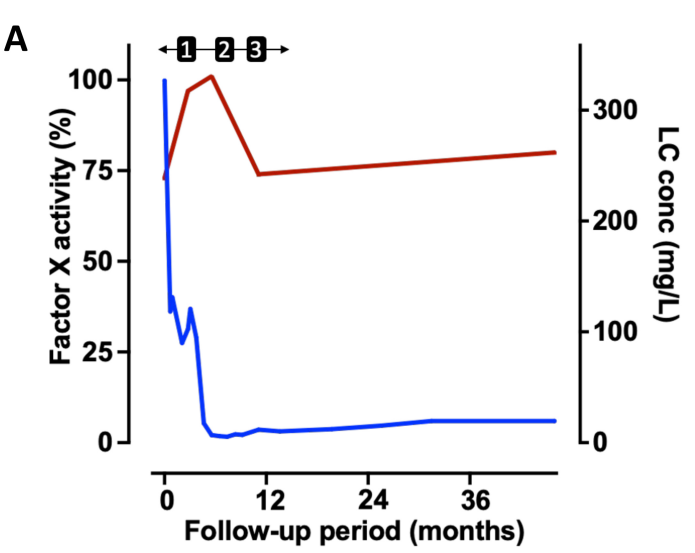
A
1 2 3
Factor X activity (%)
100
75
50
25
0
LC conc (mg/L)
300
200
100
0
0
12
24
36
Follow-up period (months)

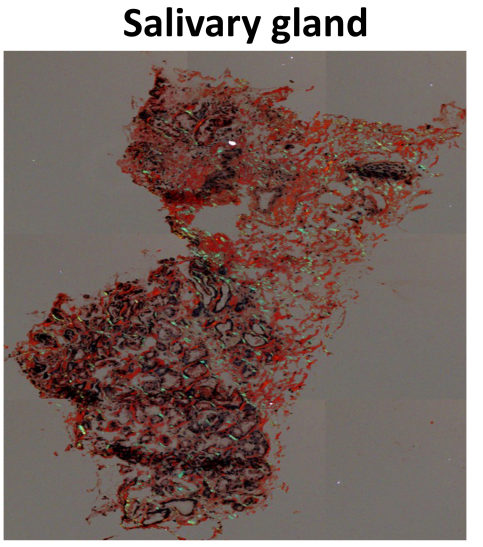
B
Salivary gland

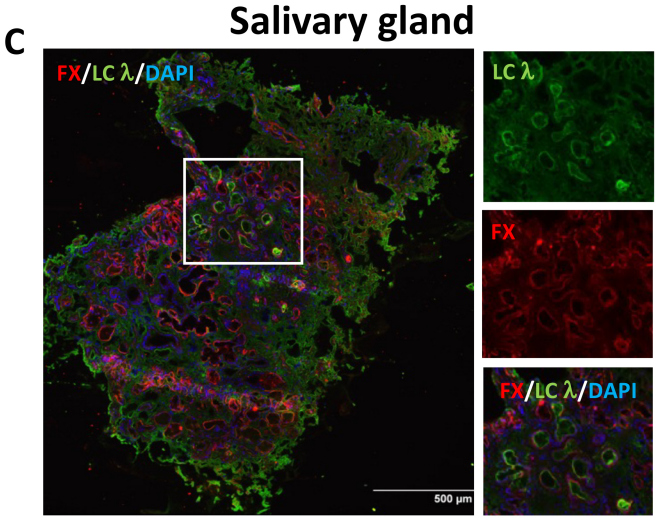
C
Salivary gland
FX/LC λ/DAPI
LC λ
FX
FX/LC λ/DAPI
500 µm

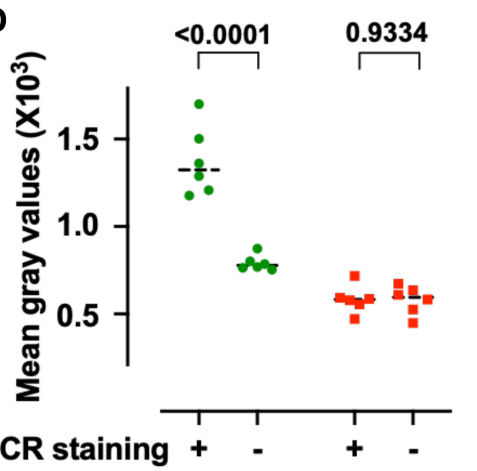
D
<0.0001
0.9334
Mean gray values (X10³)
1.5
1.0
0.5
CR staining + - + -

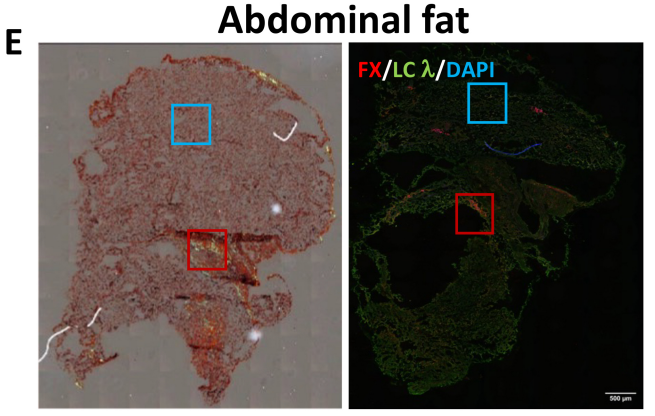
E
Abdominal fat
FX/LC λ/DAPI

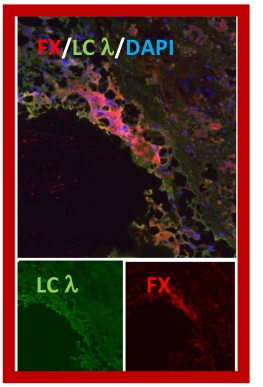
F
FX/LC λ/DAPI
LC λ
FX

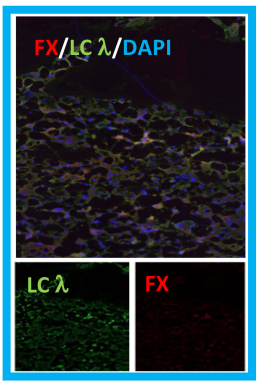
G
FX/LC λ/DAPI
LC λ
FX

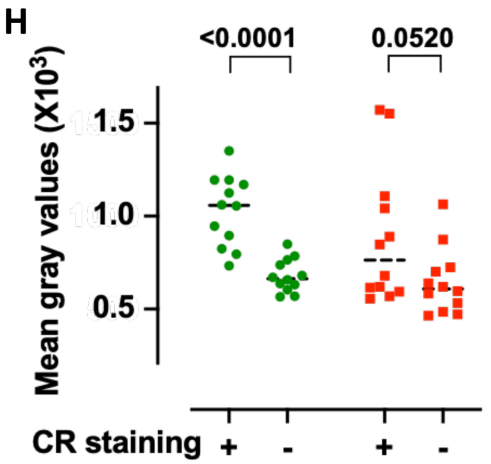
H
<0.0001
0.0520
Mean gray values (X10³)
1.5
1.0
0.5
CR staining + - + -

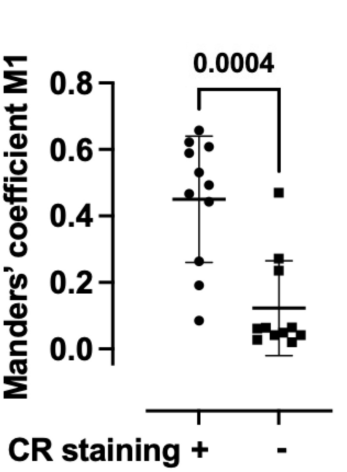
I
0.0004
Manders' coefficient M1
0.8
0.6
0.4
0.2
0.0
CR staining + -

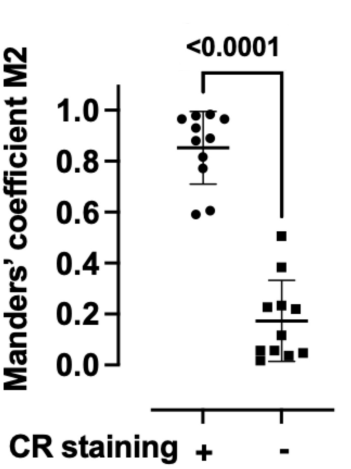
<0.0001
Manders' coefficient M2
1.0
0.8
0.6
0.4
0.2
0.0
CR staining + -

Supplementary data

Tables

Table S1. Baseline Patient Characteristics at Diagnosis or Inclusion

Characteristics	Patient 1	Patient 2	Patient 3
Age at inclusion (years)	58	71	61
Sex	M	F	M
Specific diagnosis	Indolent myeloma	MGCS	MGCS
Light chain (germline)	Kappa (Vκ1-16*02*-*Jκ5*01)	Lambda (Vl2-14*03*-*Jλ*302)	Lambda (Vλ3-1*01*-*Jλ2*01)
Cytogenetics	-	-	-
Organ Involvement	Cardiac, Digestive, Hepatic	Cardiac, Digestive, Hepatic, Neurological	Cardiac, Digestive, Neurological
Mayo 2004/European stage	II	IIIA	IIIA
Duration of monitoring (months)	77	56	44
Free light chain level (mg/L, diagnosis/ last Follow up)	110 / 36	745 / 16	326 / 20
FX:C (%,diagnosis/ last Follow up)	22 / 85	9 / 60	73 / 80
FV:C (%,diagnosis/ last Follow up)	130 / 137	130 / NM	140 / 122
FII:C (%,diagnosis/ last Follow up)	92 / 108	93 / 105	104 / 78
Anti-FX-IgG	Not Detected	Not Detected	Not Detected

Abbreviations: MGCS Monoclonal Gammopathy of Clinical Significance, FX:C, FV:C, FII:C: coagulant activities of factors X, V and II.

Table S2: Therapeutic Regimens Administered to Patients and duration.

Line of Therapy	Patient 1	Patient 2	Patient 3
1st	CyBorD (9 cycles, 8 months)	CyBorD (6 cycles, 6 months)	CyBorD (6 cycles, 6 months)
2nd	Dara/Lenalidomide/Dex (1 month)	BorD + Lenalidomide (6 months)	BorD + Dara (1 month)
3rd	Dara/Dexamethasone (6 cycles, 6 months)	-	BorD + Dara + Venetoclax (6 months) then only Venetoclax ongoing

Abbreviations: CyBorD: Cyclophosphamide, Bortezomid, Dexamethasone; BorD: Bortezomid, Dexamethasone; Dara: Daratumumab; Dex: dexamethasone.